Proton and deuteron distributions as signatures for collective particle dynamics and event shape geometries at the RHIC

B. Monreal[(a),†], W.J. Llope[(b)], R. Mattiello[(c)], S.Y. Panitkin[(d)], H. Sorge[(e)], N. Xu[(a)]

(a) Nuclear Science Division, LBNL, Berkeley, CA 94720, USA

(b) T.W. Bonner Nuclear Laboratory, Rice University, TX 77005, USA

(c) Niels Bohr Institute, Blegdamsvej 17, University of Copenhagen, DK-2100 Copenhagen, Denmark

(d) Department of Physics, Kent State University, OH 44242, USA

(e) Department of Physics, SUNY at Stony Brook, NY 11794, USA

(February 9, 2008)

We present predictions for the formation of (anti)nuclear bound states in nucleus-nucleus reactions at RHIC energies. The phase space coalescence method is used in combination with RQMD-v2.4 transport calculations to demonstrate the relevance of particle production as well as the longitudinal and transverse flow components. The formation of deuterons follows an approximate scaling law proportional to the relative freeze-out densities of nucleons and produced secondaries. For antideuterons, an additional suppression appears that is proportional to the number of nucleons, pointing toward multiple rescattering and absorption prior to freeze-out.

Nuclear clusters have been a useful tool to establish collective effects throughout the history of heavy ion reactions. Their production rates have provided evidence for low temperature phase transitions [1], their spectral distribution shows particular sensitivities to collective flow [2–4], transverse expansion [5,7–9] and potential forces [7,10]. In case of strong enough "cooling" of the emitting source and collective motion even the study of bound states with a considerable fraction of antimatter [11], strangeness or even charm [12] becomes possible. Light antimatter clusters up to $A = 3$ have already been identified [13], while the search for states with strange constituents is ongoing. Deuterons and antideuterons are the simplest composite objects and are useful in establishing expansion and correlations in the emitting source. Volume-expansion due to secondary interactions tends to diminish the cluster yields as particle production rises both with the beam energy and the system size [14]. Counterbalancing effects can be expected from collective flow components that increase cluster multiplicities and reduce effective source radii as compared to the actual size of the system [7]. It should be emphasized that the predictions of different transport models for collisions at RHIC energies already offer large differences in the most basic observables. For example, the total number of pions predicted at midrapidity varies by factors ≈ 2 in comparisons with parton cascade and RQMD-type calculations [15]. Constraints from nuclear bound state analyses (*i.e.* fragment production) should complement those from single inclusive hadron spectra

and pion/proton interferometry in order to distinguish the different model scenarios. Moreover, collective motion, temperatures and position densities are related to entropy production and pressures, major assets in the search for QCD-phase transitions. We therefore suggest cluster analyses will remain a relevant tool in the upcoming experiments at RHIC. In this paper we present predictions for (anti)proton and (anti)deuteron production based on the transport approach RQMD v2.4 [16] in combination with a phase space coalescence framework [7,9,14]. The RQMD-transport model is a semiclassical microscopic approach which combines classical propagation with stochastic interactions. Color strings and hadronic resonances can be excited in elementary collisions. Their fragmentation and decay lead to particle production. Overlapping strings may form ropes, chromoelectric flux tubes with charges in higher dimensional representations of color SU(3). RQMD is a full transport theoretical approach to reactions between nuclei and elementary hadrons. Since the model does not include light cluster production it is supplemented with a coalescence "afterburner." The coalescence is performed by projecting the 2-body phase space density given by the microscopic transport onto bound state wave functions in Wigner-space. This method has been successful in the description of deuteron formation and proton-deuteron correlations at lower beam energies [7,9,17]. The basic observables that demonstrate phase space sensitivities are the rapidity and transverse momentum distributions. Figure 1 (upper panels) shows predictions for (anti)protons and (anti)deuterons in central Au+Au collisions at full RHIC energy[1]. Fig. 1 (lower panels) presents the rapidity dependence of average transverse momenta. The values exhibit approximately a factor of two higher transverse momentum in the composite objects. The average transverse momenta of antiprotons(deuterons) are slightly larger than those of their matter counterparts. The predictions for particles and antiparticles shown in Fig. 1 are summarised in Tables 1 and 2. The presence of flow components can be

---

[1]$100 A \cdot GeV\, Au + 100 A \cdot GeV\, Au$, impact parameters $0 \leq b \leq 3$, with only participant nucleons considered.

demonstrated by comparing with calculations where the freeze-out correlations of positions and momenta have been removed by hand via randomization (crosses on Fig. 1). As a result of the randomization process the total number of clusters at midrapidity is suppressed by orders of magnitude. The average transverse momenta at midrapidity in the composite spectra drop by approximately 30%, consistent with simple momentum coalescence results. The collective component in the transverse momentum of deuterons and antideuterons is correlated with the number of scatterings: Collective expansion is highest in the midrapidity region while it becomes less pronounced close to projectile and target rapidities. A more detailed investigation of transverse flow issues can be found in Ref. [18]. In the following, ratios of particle yields are examined as measures of collectivity and (relative) freeze-out densities in longitudinal momentum. The particle yields show relatively small variations in rapidity space and the system shows strong evidence of a "collective" evolution towards freeze-out. In this case, the nuclear phase space densities can be approximated by average position densities and local momentum fluctuations, usually addressed as "temperatures". For a purely thermal source the N_d/N_p-ratio reflects the nuclear density $N_d/N_p \propto N_p/V \sim \langle \rho_p \rangle$ (where N_d is number of deuterons, N_p is number of protons, ρ_p is proton freeze-out density, V- freeze-out volume) and should not depend on the particle velocities. The transport calculations strongly deviate from such a scenario (see Fig. 2, a and c) showing N_d/N_p- and N_d/N_p^2- ratios that strongly vary as function of rapidity. This behaviour can be traced back to strong longitudinal flow components that lead to a partial separation of sources in beam direction. The effective "volume", V_p is proportional to the ratio, $\propto p^2/d$, but seems to be enlarged proportional to the number of secondaries N_{sec} (here N_{sec} is a number of produced mesons: $N_{sec} = N(\pi^{\pm,0}) + N(K^{\pm,0})$) thus supporting the role of particle production and rescattering. This can be demonstrated by regarding the "scaled" ratio $(N_d/N_p^2) * N_{sec}$ for which the differences basically vanish. In semicentral reactions less expansion is found in the N_d/N_p^2 ratio while the scaled ratio turns out to be rather similar. The comparison of reactions with different projectile or target size has been found useful to assess the relative strength of hadronic expansion at SPS-energies [14]. Such size dependences are not seen in our centrality dependence analysis although the effective nuclear volume seems to differ by factors 3-5. Note that the naive density-interpretation of the N_d/N_p ratio can be somewhat flawed by transverse and directed flow correlations which change with rapidity. Antideuterons and antiprotons reveal differing emissions patterns that are dominated by the source center. The $N_{\bar{d}}/N_{\bar{p}}$ ratio (see Fig. 2, b) is rather flat and could lead to misleading conclusions since flow correlations *appear* to be close to none. The presence of flow expresses itself in the scaled and unscaled ratios $N_{\bar{d}}/N_{\bar{p}}^2$ and $(N_{\bar{d}}/N_{\bar{p}}^2) * N_{sec}$. They are only consistent with a volume-type scaling close to midrapidity but otherwise deviate considerably. This deviation can be explained by nuclear absorption which is larger due to the presence of higher nuclear densities and lower numbers of secondaries, particularly in the domain $|y| > 3$. As a consequence, the differences become most prominent in semi-central reactions with less scattering of baryons towards midrapidity. One further suggestion to address antimatter-absorption has been suppression at low transverse momenta as well as correlations in longitudinal and transverse flow (event plane asymmetries) [11]. In agreement with such a scenario, the average transverse momenta for antinucleons are slightly larger than those for nucleons. It has been suggested [19] that the "homogeneity volume" deduced from cluster production should be compared to radius parameters extracted by HBT-type two-particle correlation analysis. We would like to point out that such an analysis suffers from major uncertainties which are related to the widths of nuclear clusters in position and momentum space. Unlike HBT-type analysis, where the correlation strength can be scanned as a function of the relative momentum of particle pairs (q_l, q_s, q_o), the projection on boundstate wave functions involves both integrations over relative momenta and positions. Hence, cluster analyses are more suitable to study the *average* phase space volume. Details of the emitting source in position space cannot uniquely be addressed unless the size and shape of the (local) momentum fluctuations are known. A solution to this caveat could be the study of various cluster types such as deuterons and ^{4}He with wave functions (correlations) very different in position and momentum space. Heavier clusters, in addition, provide less sensitivity to local momentum fluctuations than the loosely bound deuteron state. As collective flow becomes strong enough, the characteristic scaling of the relative yields can give access to the flow and density geometry ("event shape") [20]. Further insight can be expected from proton-proton and proton-deuteron correlation analysis (see for example [17]) which should confirm the shape of deuteron phase space densities. In summary, using the transport model RQMD(v2.4) and a coalescence afterburner that projects RQMD's two body phase space densities onto fragment wave functions in Wigner space, we study the production of nucleons and deuterons (and their antiparticles) for the central 100A·GeV Au + 100A·GeV Au collisions. Rapidity distributions and average transverse momentum exhibit strong longitudinal and transverse flow components. As a consequence, composite ratios are closely related to the position space distributions of the nucleons and produced hadrons close to freeze-out. Deuteron formation is consistent with a scaling relationship proportional to the relative densities of nucleons and secondaries at similar rapidities. The spectra of antideuterons are strongly modified during the course of the reaction. Contributions from antimatter absorption lead to deviations of antideuteron production from the naive volume scaling and slightly higher transverse momenta as compared to their matter counterparts.

Yet to be addressed are observables such as elliptic [21,22] or directed [7,23] flow patterns which are more sensitive to details in the early and late event shape. We are grateful for many enlightening discussions with Drs. S. Johnson, D. Keane, S. Pratt, H.G. Ritter, S. Voloshin. This research used resources of the National Energy Research Scientific Computing Center. This work has been supported by the U.S. Department of Energy under Contract No. DE-AC03-76SF00098 and W-7405-ENG-36, the Energy Research Undergraduate Laboratory Fellowship and National Science Foundation and the Marie-Curie Research Training Grant No. FMBICT961721.

† B. Monreal is at Lawrence Berkeley National Laboratory through the Center for Science and Engineering Education.

[1] J.P. Bondorf, R. Donangelo, I.N. Mishustin, H. Schultz, Nucl. Phys. **A444**, 460 (1985); J. Pochodzalla *et al.*, Phys. Rev. Lett. **75**, 1040 (1995)
[2] M.A. Lisa *et al.*, (EOS-collab.), Phys. Rev. Lett. **75**, 2662 (1995); M.D. Partlan *et al.*, (EOS-collab.), Phys. Rev. Lett. **75**, 2100 (1995)
[3] L. Ahle *et al.*, (E802-collab.), Phys. Rev. C 57, 1416 (1998)
[4] J. Barrette *et al.*, (E877-collab.), nucl-ex/9805006, subm. to Phys. Rev. C
[5] K.S. Lee, U. Heinz, Z. Phys. **C48**, 525 (1990)
[6] I.G. Bearden *et al.*, (NA44 Collab.), Phys. Rev. Lett. **78**, 2080 (1997)
[7] R. Mattiello, A. Jahns, H. Sorge, H. Stoecker, W. Greiner, Phys. Rev. Lett. **74**, 2180 (1995); R. Mattiello, H. Sorge, H. Stoecker, W. Greiner, Phys. Rev. **C55**, 1443 (1997)
[8] A. Polleri, J.P. Bondorf, I.N. Mishustin, Phys. Lett. **B419**, 19 (1998)
[9] J.L. Nagle, S. Kumar, D. Kusnezov, H. Sorge, R. Mattiello, Phys. Rev. **C53**, 367 (1996)
[10] P. Danielewicz and Q. Pan, Phys. Rev. **C46**, 2002 (1992)
[11] M.Bleicher, C. Spieles, A. Jahns, R. Mattiello, H. Sorge, H. Stoecker, W. Greiner, Phys. Lett. **B361**, 10 (1995)
[12] J. Schaffner-Bielich, C. Greiner, H. Stoecker, A.P. Vischer J.Phys. **G23**, 2107-2115 (1997) ; J. Schaffner-Bielich, A.P. Vischer, Phys.Rev. **D57**, 4142 (1998)
[13] Quark Matter '96 proceedings, Nucl. Phys. **A610**, (1996)
[14] H. Sorge, J.L. Nagle, B.S. Kumar, Phys. Lett. **B355**, 27 (1995)
[15] Talks presented on the Workshop on Transport Models at the RHIC98 Summer School, Brookhaven National Laboratory
[16] H. Sorge, Phys. Rev. **C52**, 3291 (1995)
[17] S. Panitkin, (E877 Coll.) , Proc. Int. Conf. Heavy Ion Physics at the AGS 96, eds C.A. Pruneau *et al.*, **WSU-NP-96-16**, 147 (1996)
[18] B.Monreal, *et al.* nucl-th/99904080.
[19] W.J. Llope et al., Phys. Rev. C 52, 2004 (1995); R. Scheibl and U. Heinz, PRC 59, 1585 (1999).
[20] A. Polleri, R. Mattiello, I.N. Mishustin, J.P. Bondorf, e-print nucl-th/9904012, subm. to Phys. Lett. B
[21] J.Y. Ollitrault, Phys. Rev. **D48**, 229 (1992); Phys. Rev. **D48**, 1132 (1993)
[22] H. Sorge, Phys. Rev. Lett. **78**, 2309 (1997)
[23] H. Appelshaeuser *et al.*, (NA49-collab.), Phys. Rev. Lett. **80**, 4136 (1998)

Rapidity	p	d	$\bar{p}$	$\bar{d}$
0.25	15.6	0.042	7.4	0.0092
0.75	15.9	0.049	7.1	0.0098
1.25	16.2	0.057	7.0	0.0109
1.75	16.9	0.078	6.6	0.0093
2.25	18.9	0.098	5.9	0.0095
2.75	22.0	0.150	5.1	0.0068
3.25	22.9	0.195	4.5	0.0064
3.75	21.8	0.202	4.1	0.0057
4.25	17.5	0.208	2.9	0.0049
4.75	11.3	0.159	1.0	0.0012

TABLE I. Predicted production yield for protons, deuterons, antiprotons and antideuterons as a function of rapidity.

Rapidity	p	d	$\bar{p}$	$\bar{d}$
0.25	0.89	0.69	0.93	0.72
0.75	0.90	0.67	0.97	0.73
1.25	0.88	0.67	0.96	0.71
1.75	0.87	0.65	0.93	0.68
2.25	0.84	0.63	0.92	0.66
2.75	0.80	0.59	0.86	0.58
3.25	0.73	0.53	0.80	0.59
3.75	0.66	0.45	0.73	0.47
4.25	0.58	0.37	0.62	0.35
4.75	0.49	0.30	0.54	0.40

TABLE II. Predicted mean transverse momenta (in GeV/c) for protons, deuterons, antiprotons and antideuterons as a function of rapidity.
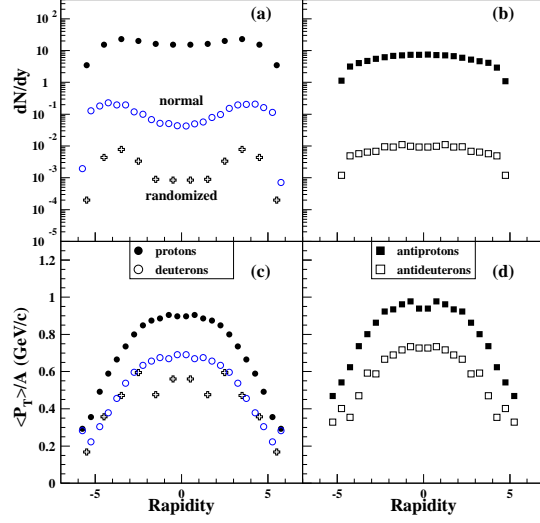
FIG. 1. Predicted rapidity distributions of **(a)** protons (filled circles), deuterons (open circles) and **(b)** anti-protons (filled squares) and anti-deuterons (open squares) for Au(200AGeV)Au reactions (b<3fm). **(c)** and **(d)** show the corresponding mean transverse momenta per nucleon as function of rapidity for protons, deuterons, antiprotons and antideuterons. Crosses indicate deuterons from calculations without position-momentum correlations in the nuclear source.
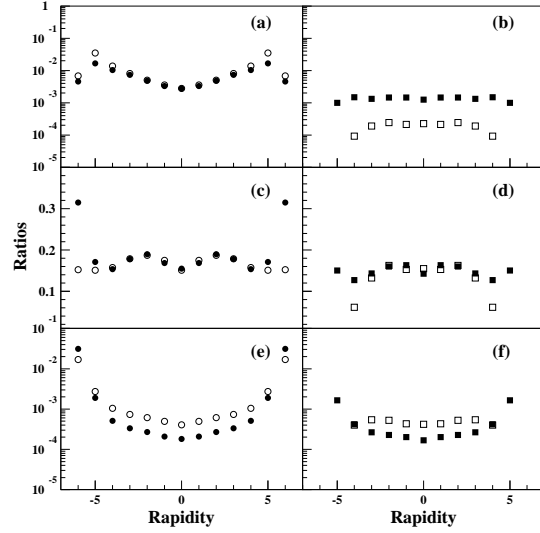

FIG. 2. Predicted ratio of particle yields as function of rapidity for central (solid symbols) and semicentral (b=6fm) events (open symbols): **(a)-(b)** N_d/N_p and $N_{\bar{d}}/N_{\bar{p}}$ ratios, **(c)-(d)** scaled ratios $(N_d/N_p^2)*N_{sec}$ and $(N_{\bar{d}}/N_{\bar{p}}^2)*N_{sec}$ and **(e)-(f)** N_d/N_p^2 and $N_{\bar{d}}/N_{\bar{p}}^2$ ratios.

4